Influence of the structure and chemical composition of tin oxide on the gas sensing properties of composite nanofibers based on multiwalled carbon nanotube

© D.V. Sokolov, S.N. Nesov, V.V. Bolotov

Omsk Scientific Center, Siberian Branch, Russian Academy of Sciences, Omsk, Russia

E-mail: classicsub-zero@mail.ru

Received May 11, 2023
Revised July 18, 2023
Accepted October 30, 2023

Individual nanofibers and thier nanobundles from multi-walled carbon nanotubes coated tin oxide were formed for two oxide compositions — amorphous and polycrystalline. Nanofibers with polycrystalline tin oxide had an increased gas response to ammonia and nitrogen dioxide by 1.4−2.8 and 2.7−3.8 times, respectively, compared to nanofibers coated amorphous nonstoichiometric oxide. The sensitivity enhance to nitrogen dioxide is explained by the additional oxidation of tin as Sn^{2+} to Sn^{4+}.

Keywords: individual nanofibers, carbon nanotube, tin oxide, gas sensitivity, chemical state.

DOI: 10.61011/PSS.2023.12.57645.5028k

The prospectivity of studying the properties of multi-walled carbon nanotubes (MWCNTs) coated with metal oxides is due to their potential use as functional elements for modern nanoelectronics, in particular, gas sensorics [1]. One of the common sensitive materials is tin oxides (SnO, SnO_2), which, depending on the structure of the films, demonstrate an increased response to gases [2]. The formation of tin oxide on the surface of individual nanotubes makes it possible to increase the degree of miniaturization of the final nanocomposite while maintaining high sensitivity to gases. Stable fixation of the oxide on the surface of the nanotube is possible by modifying the MWCNT surface by doping (with nitrogen) or introducing radiation defects (for example, irradiation with inert gas ions) [2,3]. Note that the previously presented data on the gas sensitivity of metal oxide composites were obtained mainly on massives and meshes of a large number of MWCNTs decorated with metal oxide, in particular tin [4–7]. In the presented paper the sensor properties of nanostructures based on individual modified MWCNTs coated with tin oxide with different structures and chemical compositions were studied.

Massives of nitrogen-doped MWCNTs (N-MWCNTs) were synthesized by CVD method by pyrolysis of acetonitrile in an argon flow at 800°C. The catalyst for the growth of nanotubes on SiO_2/Si substrate was iron nanoparticles formed from ferrocene. For this purpose, ferrocene was added to acetonitrile in a ratio of 1 : 100. To modify the surface of nanotubes, the initial N-MWCNT massives were irradiated with argon ions with an energy of 15 keV for 15 min, the total dose was 10^{16} cm^{-2}. Tin oxide on the surface of irradiated MWCNTs was formed by magnetron sputtering of metal tin target in two modes: 1) in an argon atmosphere at pressure of 0.1 Pa with a discharge power of 50 W; 2) in mixture of $Ar + O_2$ at pressure of 0.85 Pa with a discharge power of 70 W.

The morphology of the nanocomposites was analyzed using images obtained on JEOL JSM-6610 LV scanning electron microscope (SEM). The structure of nanocomposite massives was studied using X-ray absorption fine structure spectroscopy at BESSY II synchrotron radiation center.

Individual tin oxide/N-MWCNT nanotubes and nanofibers were deposited from a suspension of the synthesized nanocomposite in dichloromethane onto a matrix of gold microelectrodes by spin-coating. MFP-3D SA atomic force microscope (AFM) (Asylum Research) was used to detect individual nanotubes and tin oxide-coated nanofibers located between two measured microelectrodes. Current-voltage curves were recorded using Agilent E4980A LCR Meter.

To reveal the gas sensitivity of nanostructures the measurements were carried out in a closed cell with a volume of 6 ml in a flow of dry nitrogen (speed 0.5−1 mL/s). When the relative humidity reached at least 5−8%, the following gases with a concentration of 500 ppm were introduced into the cell: CO, NO_2, NH_3 and H_2S. The longitudinal resistance of nanofibers during gas adsorption was measured with AM-1038 digital device at voltages +0.5 and +1 V. The gas response (S) was defined as the relative change in the resistance of nanostructures in a flow of dry nitrogen before (R_0) and after (R) exposure to the analyzed gas: $S = (R_0 - R)/R_0$. For each gas 5−12 samples of three types were used, the final values were averaged.

The ultra-soft X-ray absorption spectra of the Sn M-edge for the composites under study differ significantly (Figure 1, curves *1* and *2*). The spectrum of composite formed using reaction gas (Figure 1, curve *2*) has characteristic spectral features of the fine structure of M_5- and M_4-absorption edges (designated as *a, b, c* and *d, e*, respectively), present in the spectrum of the reference powder SnO with natural

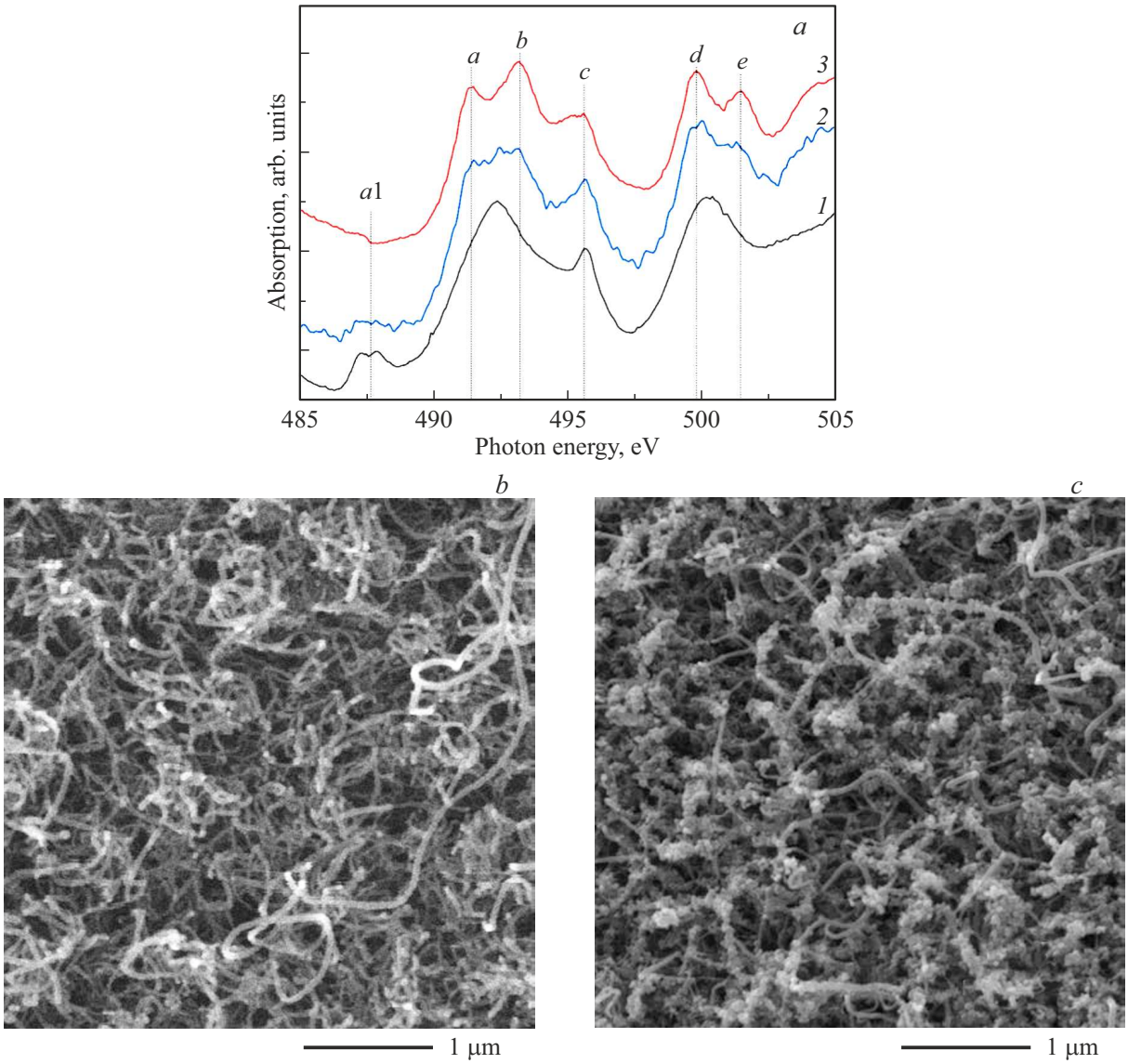

Figure 1. X-ray absorption fine structure spectra of samples (*a*): *1* — SnO_x/N-MWCNT; *2* — SnO/N-MWCNT; *3* — standard SnO powder; SEM images of SnO_x/N-MWCNT (*b*) and SnO/N-MWCNT (*c*) massives.

oxide (Figure 1, curve *3*). This indicates a polycrystalline structure of tin oxide with chemical composition close to stoichiometric SnO in this composite (SnO/N-MWCNTs).

However, the presence of a spectral feature in the region of low photon energies (a1), associated with the presence of oxygen vacancies [8], as well as a more diffuse fine structure of the absorption spectrum, compared to the spectrum of the standard, indicates the defectiveness of tin monoxide in the composite SnO/N-MWCNTs (Figure 1, curves *2* and *3*).

The spectrum of the composite formed without the reaction gas use (Figure 1, curve *1*) does not have the fine structure characteristic of crystalline tin oxides. Spectral feature a1 has a high relative intensity, which indicates a significant deficiency of oxygen in the composition of the metal oxide layers covering MWCNTs (SnO_x/N-MWCNTs, where $x = 1-2$) [8].

In addition, the two types of nanocomposites have different morphologies — in SnO_x/N-MWCNT oxide covers the nanotubes with continuous layer (Figure 1, *b*), in SnO/N-MWCNTs polycrystalline oxide conglomerates are observed (Figure 1, *c*).

According to AFM images, the nanostructures were individual nanofibers (Figure 2, *a*, insert) or bundles of 2–4 nanofibers. The average diameters of individual nanotubes and composite nanofibers were 22–35 and 41–55 nm, respectively, which confirms the presence of oxide layer on the N-MWCNTs surface. The ends of the nanofibers have fairly stable contact with the electrodes and do not move during AFM scanning and gas-sensitive measurements.

In all cases, the current-voltage curves of the resulting nanostructures had a symmetrical appearance with weak

Table 1. Average values and scatterings of longitudinal resistance and gas response for individual nanotubes and composite nanofibers

Sample	R_0, MΩ	S, %			
		NH_3	NO_2	H_2S	CO
Irradiated N-MWCNT	0.1–0.8	-6.6 ± 1.8	8.1 ± 2.1	7.1 ± 4.7	-1.4 ± 0.3
SnO_x/N-MWCNT	4.0–12.0	-7.4 ± 0.2	10.6 ± 2.3	-8.9 ± 2.1	-0.6 ± 0.3
SnO/N-MWCNT	0.4–2.3	-16.3 ± 5.4	37.5 ± 11.4	-3.5 ± 2.2	-0.5 ± 0.2

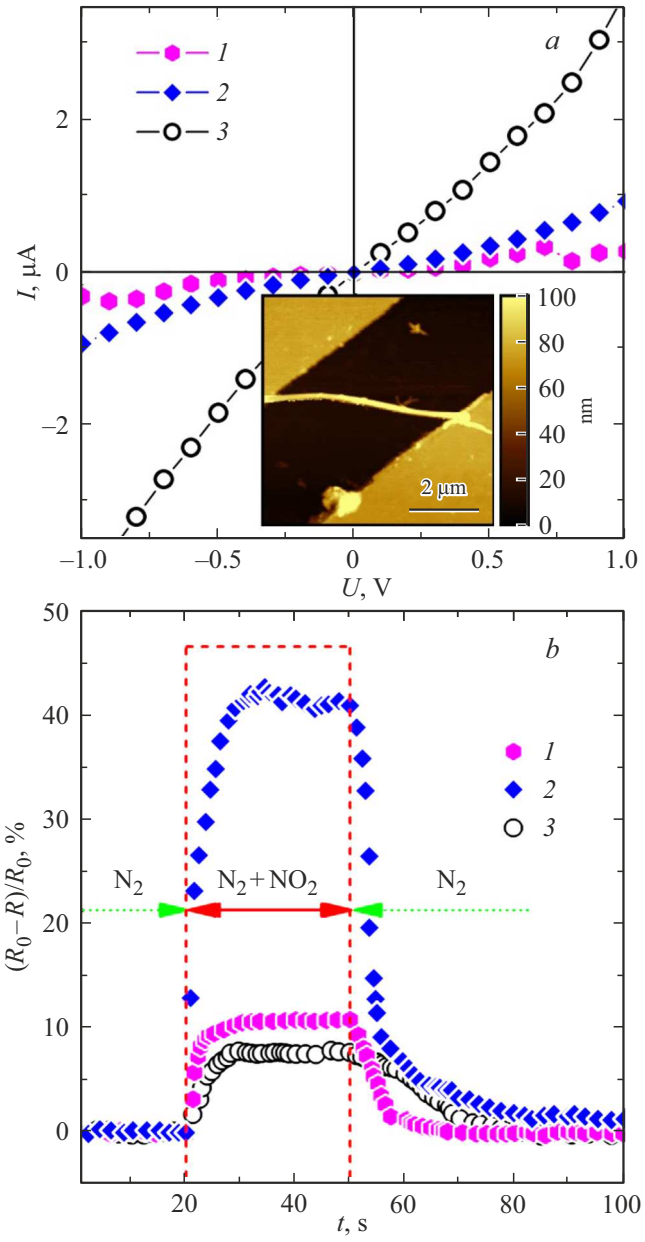

Figure 2. Current-voltage curves with insertion of AFM image of individual nanofiber SnO_x/N-MWCNT (*a*) and the dynamics of changes in the gas response to 500 ppm NO_2 (*b*): *1* — SnO_x/N-MWCNT; *2* — SnO/N-MWCNT; *3* — irradiated N-MWCNT.

nonlinearity (Figure 2, *a*), which indicates the tunneling transport of charge carriers through the barriers of „tin oxide/nanotube/gold“ transitions.

The dynamics of resistance changes during exposure in gases has a classical exponential dependence (Figure 2, *b*). For all samples, the response and recovery times were ∼ 10 and 30 s, respectively. Since for nanotubes and semiconductor oxides the molecules NH_3 (NO_2) exhibit reducing (oxidizing) properties, the adsorption of the corresponding gas shall lead to a decrease (increase) in the resistance of the conductor of *p*-type. This confirms that holes are the main charge carriers in nanotubes and composite nanofibers.

The adsorption of CO molecules on all samples is almost the same (does not exceed ∼ 2%) and is not considered further. The absolute values of the gas response of SnO_x/N-MWCNTs and SnO/N-MWCNTs to NH_3 and NO_2 are greater relative to the initial nanotubes by 1.0–1.3 and 2.2–8.2 times, respectively (Table 1). Compared to SnO_x/N-MWCNTs, the gas response in SnO/N-MWCNT nanofibers to H_2S is by 2.5–7.8 times smaller, and to NH_3 by 1.4–2.8 times greater. In this case, exposure to NO_2 gives by 2.7–3.8 times greater response of SnO/N-MWCNTs than for SnO_x/N-MWCNTs.

It was found that the effect of reducing gas H_2S on irradiated N-MWCNTs possessing *p*-type of conductivity [9] demonstrates a decrease in resistance, in contrast to composite nanofibers. To explain the differences in sensitivity and selectivity to gases of nanotubes and composite nanofibers, it is necessary to consider the energy band diagram according to the literature data as per their energy characteristics (Table 2). As can be seen, the values of the work function φ in irradiated N-MWCNTs and SnO_x are almost equal and differ slightly from gold. The electron affinity energy χ for MWCNTs and SnO_x critically depends on the degree of their defectiveness, and in the literature is presented mainly for materials of *n*-type conductivity. Experimental studies show the absence of band gap E_g for MWCNTs, but theoretically the values E_g can only be determined in the outer layer of the nanotube [10].

According to the selected parameters of the band structure of the materials used, for all three cases a contact layer with increased conductivity is formed at the boundary of the gold electrode in semiconductors (Figure 3). Consequently, $I-V$ curves nonlinearity may be due to the presence of a thin layer of adsorbate, forming intermediate energy barrier. For N-MWCNT/Au and SnO_x/Au, the nature of the band

Table 2. Energy parameters of the band structure

Component	φ, eV	χ, eV	E_g, eV
Irradiated N-MWCNT	4.86 [9]	–	1.40 [10]
SnO_x	4.80 [11]	–	2.35 [11]
SnO	4.10 [12]	3.50 [13]	0.70 [13]
Au	4.90 [14]	–	–

bending is almost the same, as are the absolute values of the response (Table 1). Adsorption of H_2S on N-MWCNTs can lead to bending of the conduction band closer to the Fermi level and change in the type of main charge carriers. Under further gas effect the nanotubes behave like a *n*-type semiconductor, resulting in the resistance decreasing.

The greatest band bending occurs in the SnO/Au heterojunction, in which the parameters of the tunnel barrier will more significantly reflect the change in the resistance of the nanofiber in gas atmosphere. The additional contribution to the increase in sensitivity is the potential barriers between SnO crystallites, which determine the final resistance of the polycrystal [15]. Maximum response of SnO/N-MWCNT to NO_2 can be associated with tin oxidation: $Sn^{2+} + 2NO_2 = Sn^{4+} + 2NO_2^-$. This leads to a significant increase in the resistance of nanofibers, since the average resistance of SnO_x/N-MWCNTs is by 2–4 times greater than that of SnO/N-MWCNTs (Table 1). Similarly, the reduced response to H_2S for SnO/N-MWCNTs can be determined by the tin reduction reaction, which occurs predominantly in SnO_x.

Thus, the oxygen use in the reaction mixture makes it possible to obtain polycrystalline form of tin (II) oxide on the surface of nanotubes. Without the oxygen addition nonstoichiometric SnO_x (SnO/SnO_2) is formed. Coating N-MWCNTs with polycrystalline tin (II) oxide increases the response to NH_3 and NO_2 by 2.5–4.0 and 3.1–8.2 times, respectively. The maximum response of individual SnO/N-MWCNT nanofibers to NO_2 may be associated with the tin oxidation to Sn (IV) with higher resistivity. The sizes of the obtaining nanofibers allow their use as a selective element for NO_2 in gas nanosensors.

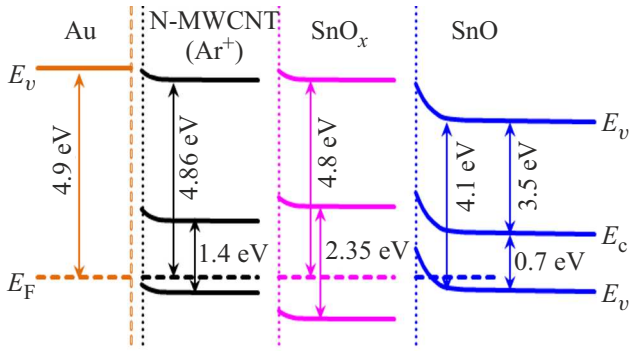

Figure 3. Bends of energy levels in various types of nanofibers at the interface with a gold electrode.

Acknowledgments

The authors are grateful to K.E. Ivlev for his assistance in obtaining SEM images.

Funding

The study was carried out according to the state assignment of the Omsk Scientific Center of the Siberian Branch of the Russian Academy of Sciences (state registration number 121021600004-7). The study was carried out using the equipment of the Omsk Regional Center for Collective Use of the Siberian Branch of the Russian Academy of Sciences.

Conflict of interest

The authors declare that they have no conflict of interest.

References

[1] P. Dariyal, S. Sharma, G.S. Chauhan, B.P. Singh, S.R. Dhakate. Nanoscale Adv. **3**, 6514 (2021).
[2] A.V. Sitnikov, O.V. Zhilova, I.V. Babkina, V.A. Makagonov, Yu.E. Kalinin, O.I. Remizova. FTP **52**, *9*, 995 (2018). (in Russian).
[3] J.A. Lee, W.J. Lee, J. Lim, S.O. Kim. Nanomaterials **11**, 1882 (2021).
[4] S.N. Nesov, P.M. Korusenko, V.A. Sachkov, V.V. Bolotov, S.N. Povoroznyuk, J. Phys. Chem. Solids **169**, 110831 (2022).
[5] Z.N. Adamyan, A.G. Sayunts, E.A. Khachaturyan, V.M. Aroutiounian, S. Florida J. Develop. **2**, *1*, 1066 (2021).
[6] Q.T.M. Nguyet, N.V. Duy, C.M. Hung, N.D. Hoa, N.V. Hieu. App. Phys. Lett. **112**, *15*, 153110 (2018).
[7] P. Tyagi, A. Sharma, M. Tomar, V. Gupta. Sens. Actuators B **248**, 980 (2017).
[8] M.D. Manyakin, S.I. Kurganskii, O.I. Dubrovskii, O.A. Chuvenkova, E.P. Domashevskaya, S.V. Ryabtsev, R. Ovsyannikov, E.V. Parinova, V. Sivakov, S.Y. Turishchev. Mater Sci. Semicond. Proc. **99**, 28 (2019).
[9] N.A. Davletkildeev, D.V. Sokolov, E.Yu. Mosur, V.V. Bolotov. IOP Conf. Ser.: Mater. Sci. Eng. **699**, 012010 (2019).
[10] N.G. Bobenko, V.V. Bolotov, V.E. Egorushkin, P.M. Korusenko, N.V. Melnikova, S.N. Nesov, A.N. Ponomarev, S.N. Povoroznyuk. Carbon **153**, 40 (2019).
[11] L. Grządziel, M. Krzywiecki, A. Szwajca, A. Sarfraz, G. Genchev, A. Erbe. J. Phys. D **51**, *31*, 315301 (2018).
[12] S. Ullah, G. Wan, C. Kouzios, C. Woodgate, M. Cattelan, N. Fox. Appl. Surf. Sci. **559**, 149962 (2021).
[13] J. Wang, N. Umezawa, H. Hosono. Adv. Energy Mater. **6**, *1*, 1501190 (2016).
[14] D.V. Sokolov, V.V. Bolotov, Y.A. Stenkin, K.E. Ivlev. AIP Conf. Proc. **2412**, 040006 (2021).
[15] Y. Kong, Y. Li, X. Cui, L. Su, D. Ma, T. Lai, L. Yao, X. Xiao, Y. Wang, Nano Mater Sci., **4**, *4*, 339 (2021).

Translated by I.Mazurov